

Monte Carlo reconstruction of the inflationary potential

Richard Easther* and William H. Kinney†
Institute for Strings, Cosmology and Astroparticle Physics
Columbia University
550 W. 120th St., New York, NY 10027
(Dated: October 15, 2002)

We present Monte Carlo reconstruction, a new method for “inverting” observational data to constrain the form of the scalar field potential responsible for inflation. This stochastic technique is based on the flow equation formalism and has distinct advantages over reconstruction methods based on a Taylor expansion of the potential. The primary ansatz required for Monte Carlo reconstruction is simply that inflation is driven by a single scalar field. We also require a very mild slow roll constraint, which can be made arbitrarily weak since Monte Carlo reconstruction is implemented at arbitrary order in the slow roll expansion. While our method cannot evade fundamental limits on the accuracy of reconstruction, it can be simply and consistently applied to poor data sets, and it takes advantage of the attractor properties of single-field inflation models to constrain the potential outside the small region directly probed by observations. We show examples of Monte Carlo reconstruction for data sets similar to that expected from the Planck satellite, and for a hypothetical measurement with a factor of five better parameter discrimination than Planck.

PACS numbers: 98.80.Cq

I. INTRODUCTION

Given a detailed model of physics at the Grand Unified Theory (GUT) scale that supports inflation one can deduce many of the overall properties of the universe from first principles. However, new strides in precision cosmology are likely to present us with the inverse problem: given an accurate measurement of the primordial perturbation spectrum, can we determine the particle physics that drove inflation? This question leads to “reconstruction” – rebuilding a portion of the inflationary potential from observations – whose apotheosis is the work of Lidsey et al. [1]. The conclusion of this effort was that while a limited reconstruction may be possible, it is overly optimistic to hope to deduce more than the rough form of a small piece of the inflaton potential on the basis of astrophysical observations alone.

Despite this apparent setback, the prospect of being able to probe ultra-high energy particle physics via astrophysical measurements remains tempting. In this paper we present a new approach to the task, *Monte Carlo reconstruction*. Unlike previous workers, we tackle the problem stochastically, by generating large numbers of inflationary models and their associated potentials and identifying those that lead to a spectrum of primordial perturbations which fits inside a specified window of parameter space. We sacrifice the prospect of unambiguously reconstructing the inflationary potential, but instead map out the ensemble of viable potentials. We can then assess the extent to which these potentials resemble one another, and thus the degree of ambiguity in the

“reconstruction”.

The starting point for Monte Carlo reconstruction is the Hubble slow roll expansion [2], which leads to a set of first order “flow” equations [3, 4] that describes the inflationary dynamics. The Hubble slow roll expansion can be systematically continued to arbitrary order but, as we explain below, the truncated expansion actually yields an exact solution of the full equations, drawn from a subset of the overall solution space. We select a “universe” by assigning random values to each term in the truncated slow roll expansion, and integrate the flow equations forward to the end of inflation (or far enough into the future to show that the solution approaches an inflationary attractor). We can then determine the epoch that corresponds to cosmological structure formation and thus the predicted parameters of the primordial spectrum, allowing us to select the models which fit into a pre-determined window of parameter space.

As with any other reconstruction program, we face limitations dictated by the physics of inflation itself. Since the field rolls slowly, it traverses only a small portion of the potential during the epoch in which the primordial perturbations are laid down. Consequently, even if all the potentials we recover for a specific set of cosmological parameters overlap in the region where the cosmologically relevant portion of the spectrum is laid down, they will still diverge outside this region. However, because we reconstruct the entire potential, we can estimate the degree to which the reconstructed potentials diverge from one another.

In the following section we summarize the inflationary dynamics and the flow equations, and in Section 3 apply these to spell out the process of Monte Carlo reconstruction in detail. We present the results of a variety of simulations in Section 4, and test how accurately Monte Carlo reconstruction can recover a known inflationary po-

*Electronic address: easther@physics.columbia.edu

†Electronic address: kinney@physics.columbia.edu

tential. As expected, a fully consistent reconstruction requires the unambiguous detection of tensor modes in the CMB, but even in the absence of a detectable tensor signal we can still recover some information about the inflationary potential. If we assume the error bars on the scalar spectral index and tensor-to-scalar ratio that are expected for the Planck mission, the underlying potential cannot be unambiguously recovered. However, if we decrease these error bars (perhaps by adding information from large scale structure surveys, or better measurements of CMB polarization) by a factor of 5, then we can start to recover a ϕ^n potential. Our conclusions are summarized in Section 5.

II. INFLATION AND FLOW

We consider inflation driven by a single homogeneous scalar field ϕ (the *inflaton*) with potential $V(\phi)$ and equation of motion

$$\ddot{\phi} + 3H\dot{\phi} + V'(\phi) = 0, \quad (1)$$

where $H \equiv (\dot{a}/a)$ is the Hubble parameter. We assume a spatially flat, homogeneous and isotropic universe where the inflaton field is the only contribution to the energy-momentum tensor, so that the Einstein field equations have the familiar form

$$H^2 = \left(\frac{\dot{a}}{a}\right)^2 = \frac{8\pi}{3m_{\text{Pl}}^2} \left[V(\phi) + \frac{1}{2}\dot{\phi}^2 \right], \quad (2)$$

and

$$\frac{\ddot{a}}{a} = \frac{8\pi}{3m_{\text{Pl}}^2} \left[V(\phi) - \dot{\phi}^2 \right]. \quad (3)$$

Here $m_{\text{Pl}} = G^{-1/2} \simeq 10^{19}$ GeV is the Planck mass. These background equations, along with the equation of motion (1), form a coupled set of differential equations that describe the evolution of the universe. The limit $\dot{\phi} = 0$ corresponds to a de Sitter universe, with the scale factor increasing exponentially in time

$$H = \sqrt{\left(\frac{8\pi}{3m_{\text{Pl}}^2}\right) V(\phi)} = \text{const}, \quad a \propto e^{Ht}. \quad (4)$$

In general H is not exactly constant, but varies as the field ϕ evolves along the potential $V(\phi)$. A powerful way of describing the dynamics of an inflationary universe with a varying field (and non-trivial potential) is to express the Hubble parameter as a function of the field ϕ , $H = H(\phi)$, which is consistent provided ϕ is monotonic in time. The equations of motion become [1, 5, 6, 7]

$$\begin{aligned} \dot{\phi} &= -\frac{m_{\text{Pl}}^2}{4\pi} H'(\phi), \\ [H'(\phi)]^2 - \frac{12\pi}{m_{\text{Pl}}^2} H^2(\phi) &= -\frac{32\pi^2}{m_{\text{Pl}}^4} V(\phi). \end{aligned} \quad (5)$$

These are completely equivalent to the second-order equation of motion (1). The second of the above equations is referred to as the *Hamilton-Jacobi* equation, and can be written in the useful form

$$H^2(\phi) \left[1 - \frac{1}{3}\epsilon(\phi) \right] = \left(\frac{8\pi}{3m_{\text{Pl}}^2} \right) V(\phi), \quad (6)$$

where ϵ is defined to be

$$\epsilon \equiv \frac{m_{\text{Pl}}^2}{4\pi} \left(\frac{H'(\phi)}{H(\phi)} \right)^2. \quad (7)$$

The physical meaning of ϵ can be seen by expressing Eq. (3) as

$$\left(\frac{\ddot{a}}{a} \right) = H^2(\phi) [1 - \epsilon(\phi)], \quad (8)$$

so that the condition for inflation ($\ddot{a}/a > 0$) is given by $\epsilon < 1$. The scale factor is given by

$$a \propto e^N = \exp \left[\int_{t_0}^t H dt \right], \quad (9)$$

where the number of e-folds N is

$$N \equiv \int_t^{t_e} H dt = \int_{\phi}^{\phi_e} \frac{H}{\dot{\phi}} d\phi = \frac{2\sqrt{\pi}}{m_{\text{Pl}}} \int_{\phi_e}^{\phi} \frac{d\phi}{\sqrt{\epsilon(\phi)}}. \quad (10)$$

It is convenient to use N as the measure of time during inflation. We take t_e and ϕ_e to be the time and field value at end of inflation. Therefore N is defined as the number of e-folds before the end of inflation and increases as one goes *backward* in time, $dt > 0 \Rightarrow dN < 0$. The sign convention for $\sqrt{\epsilon}$ must be applied carefully, and we take it to have the same sign as $H'(\phi)$:

$$\sqrt{\epsilon} \equiv +\frac{m_{\text{Pl}}}{2\sqrt{\pi}} \frac{H'}{H}. \quad (11)$$

Liddle, Parsons and Barrow use this as the starting point for an infinite hierarchy of slow roll parameters [2]:

$$\begin{aligned} \sigma &\equiv \frac{m_{\text{Pl}}}{\pi} \left[\frac{1}{2} \left(\frac{H''}{H} \right) - \left(\frac{H'}{H} \right)^2 \right], \\ {}^\ell \lambda_{\text{H}} &\equiv \left(\frac{m_{\text{Pl}}^2}{4\pi} \right)^\ell \frac{(H')^{\ell-1}}{H^\ell} \frac{d^{(\ell+1)} H}{d\phi^{(\ell+1)}}. \end{aligned} \quad (12)$$

The evolution of these parameters during inflation is determined by a set of “flow” equations [3, 4],

$$\begin{aligned} \frac{d\epsilon}{dN} &= \epsilon(\sigma + 2\epsilon), \\ \frac{d\sigma}{dN} &= -5\epsilon\sigma - 12\epsilon^2 + 2({}^2\lambda_{\text{H}}), \\ \frac{d({}^\ell \lambda_{\text{H}})}{dN} &= \left[\frac{\ell-1}{2}\sigma + (\ell-2)\epsilon \right] ({}^\ell \lambda_{\text{H}}) + {}^{\ell+1}\lambda_{\text{H}}. \end{aligned} \quad (13)$$

Here the time variable is the number of e-folds N , where

$$\frac{d}{dN} = \frac{d}{d \log a} = \frac{m_{\text{Pl}}}{2\sqrt{\pi}} \sqrt{\epsilon} \frac{d}{d\phi}. \quad (14)$$

The derivative of a slow roll parameter at a given order is higher order in slow roll. Taken to infinite order, this set of equations completely specifies the cosmological evolution, up to the normalization of the Hubble parameter H . When truncated at *finite* order, by assuming that the ${}^\ell \lambda_H$ are all zero above some fixed value of ℓ , the solution of the flow equations still yields an *exact* solution of the background equations, albeit one that is drawn from a special subset of the overall solution space.

III. MONTE CARLO RECONSTRUCTION

The inflationary dynamics are fully specified by the values of the slow roll parameters $[\epsilon, \sigma, {}^\ell \lambda_H]$ at a fixed time, which serve as initial conditions for the flow equations, truncated at order M in the slow roll expansion. We now show that this information determines the inflationary potential $V(\phi)$, up to a constant multiplier. The starting point is the Hamilton-Jacobi equation,

$$V(\phi) = \left(\frac{3m_{\text{Pl}}^2}{8\pi} \right) H^2(\phi) \left[1 - \frac{1}{3} \epsilon(\phi) \right]. \quad (15)$$

We have $\epsilon(N)$ trivially from the flow equations. In order to calculate the potential, we need to determine $H(N)$ and $\phi(N)$. With ϵ known, $H(N)$ can be determined by inverting the definition of ϵ , Eq. (7):

$$\frac{1}{H} \frac{dH}{dN} = \epsilon. \quad (16)$$

This can be viewed as the lowest-order member of the system of flow equations (13). Similarly, $\phi(N)$ follows from the first Hamilton-Jacobi equation (5):

$$\frac{d\phi}{dN} = \frac{m_{\text{Pl}}}{2\sqrt{\pi}} \sqrt{\epsilon}. \quad (17)$$

Using these equations and Eq. (15), the form of the potential can then be fully reconstructed from the numerical solution for $\epsilon(N)$.¹ The only necessary observational input is the normalization of the Hubble parameter H , which enters the above equations as an integration constant. Here we use the simple condition that the density fluctuation amplitude (as determined by a first-order slow roll expression) be of order 10^{-5} ,

$$\frac{\delta\rho}{\rho} \simeq \frac{H}{2\pi m_{\text{Pl}} \sqrt{\epsilon}} = 10^{-5}. \quad (18)$$

¹ Expressing the potential in this way is certainly not new. This is the basis of “functional reconstruction” method of Refs. [8, 9], and well as the “Stewart-Lyth inverse problem” of Ref. [10].

A more sophisticated treatment would perform a full normalization to the COBE CMB data [11, 12]. The value of the field, ϕ , also contains an arbitrary, additive constant.

Given a solution to the flow equations it is straightforward to determine the observational predictions for that model, even before the potential is computed. For instance, measurements of CMB anisotropies [13, 14] may determine the tensor/scalar ratio r , the spectral index n , and the “running” of the spectral index $dn/d \log k$, and we focus on these quantities here. To lowest order, the relationship between the slow roll parameters and the observables is especially simple: $r = \epsilon$, $n - 1 = \sigma$, and $dn/d \log k = 0$. To second order in slow roll, the observables are given by [2, 15],

$$r = \epsilon [1 - C(\sigma + 2\epsilon)], \quad (19)$$

for the tensor/scalar ratio, and

$$n - 1 = \sigma - (5 - 3C)\epsilon^2 - \frac{1}{4}(3 - 5C)\sigma\epsilon + \frac{1}{2}(3 - C)({}^2\lambda_H) \quad (20)$$

for the spectral index. The constant $C \equiv 4(\ln 2 + \gamma)$, where $\gamma \simeq 0.577$ is Euler’s constant. Derivatives with respect to wavenumber k can be expressed in terms of derivatives with respect to N as [21]

$$\frac{d}{dN} = -(1 - \epsilon) \frac{d}{d \ln k}, \quad (21)$$

The scale dependence of n is then given by the simple expression

$$\frac{dn}{d \ln k} = - \left(\frac{1}{1 - \epsilon} \right) \frac{dn}{dN}, \quad (22)$$

which can be evaluated to third order in slow roll by using Eq. (20) and the flow equations. The final result following the evaluation of a particular path in M dimensional “slow roll space” is a point in “observable parameter space”, i.e. $(r, n, dn/d \log k)$, corresponding to the observational prediction for that particular model. This process can be repeated for a large number of models, and used to study the attractor behavior of the inflationary dynamics. In fact, the models cluster strongly in the observable parameter space [3].

We are now in a position to ask the key question: given an observational constraint, what dynamics – and underlying inflationary potential – are compatible with that constraint? We proceed by generating a large number of “universes” with random values (in a sense that is made explicit below) for the slow roll parameters. Given an allowed region in the observable parameter space, centered on specified values of r, n , and $dn/d \log k$ with a width given by the error bars on these quantities, we can construct an ensemble of inflationary potentials consistent with the specified “window” in parameter space. This Monte Carlo approach to reconstruction differs from previously used techniques [1, 16, 17] in that it generates an ensemble of potentials consistent with a

given constraint, rather than attempting to produce a parameterized form for the potential and then constrain those parameters. The advantage of Monte Carlo reconstruction is that by evaluating the flow equations to high enough order we need only very mild *a priori* assumptions about the form of the potential. In addition, by probing the parameter space in a uniform way, we obtain what is in some sense a “fair sample” of the potentials consistent with a given observational bound. Even so, we do not have a metric on the space of initial conditions, so it is not possible to derive statistical inferences from the ensemble of potentials.

The condition for the end of inflation is that $\epsilon = 1$. Integrating the flow equations forward in time will yield two possible outcomes. One possibility is that the condition $\epsilon = 1$ may be satisfied for some finite value of N , which defines the end of inflation. We identify this point as $N = 0$ so that the primordial fluctuations are actually generated when $N \sim 50$. Alternatively, the solution can evolve toward an inflationary attractor with $r = 0$ and $n > 1$, in which case inflation never stops.² In reality, inflation must stop at some point, presumably via some sort of phase transition, such as the “hybrid” inflation mechanism [18, 19, 20]. Here we make the simplifying assumption that the observables for such models are the values at the late-time attractor.

To summarize, the algorithm for Monte Carlo reconstruction is as follows:

1. Specify a “window” of parameter space: e.g. central values for $n - 1$, r or $dn/d \ln k$ and their associated error bars.
2. Select a random point in slow roll space, $[\epsilon, \eta, {}^\ell \lambda_H]$, truncated at order M in the slow roll expansion.
3. Evolve forward in time ($dN < 0$) until either (a) inflation ends ($\epsilon > 1$), or (b) the evolution reaches a late-time fixed point ($\epsilon = {}^\ell \lambda_H = 0$, $\sigma = \text{const.}$)
4. If the evolution reaches a late-time fixed point, calculate the observables r , $n - 1$, and $dn/d \ln k$ at this point.
5. If inflation ends, evaluate the flow equations backward N e-folds from the end of inflation. Calculate the observable parameters at this point.
6. If the observable parameters lie within the specified window of parameter space, compute the potential and add this model to the ensemble of “reconstructed” potentials.
7. Repeat steps 2 through 6 until the desired number of models have been found.

In principle it is possible to carry out Monte Carlo reconstruction with no assumptions about the convergence of the hierarchy of slow roll parameters. In practice, the flow equations (13) must be truncated at some finite order and evaluated numerically. Moreover, for any given path in the parameter space, we do not know *a priori* the correct number of e-folds N at which to evaluate the observables, since this depends on details such as the energy density during inflation and the reheat temperature [1]. Consequently, after truncating to order M in slow roll, we select our models’ parameters randomly from the following uniform distributions:

$$\begin{aligned} N &= [40, 70] \\ \epsilon &= [0, 0.8] \\ \sigma &= [-0.5, 0.5] \\ {}^2\lambda_H &= [-0.05, 0.05] \\ {}^3\lambda_H &= [-0.025, 0.025], \\ &\dots \\ {}^{M+1}\lambda_H &= 0. \end{aligned} \tag{23}$$

and so forth, reducing the width of the range by factor of five for each higher order in slow roll. The series is closed to order M by taking ${}^{M+1}\lambda_H = 0$. We use $M = 5$ for the calculations in this paper. The exact choice of ranges for the initial parameters does not have a large influence on the result of the Monte Carlo process, as long as they are chosen such that the slow roll hierarchy is convergent. As noted above, the form of the flow equations (13) ensures that the derivative of ${}^\ell \lambda_H$ depends only on parameters of order ℓ and $\ell + 1$, so this truncation still leads to an *exact* evaluation of the flow equations to infinite order. We are selecting a finite subset out of an infinite number of possibilities for initial conditions, but the background evolution for a given model is evaluated exactly.³

The result of integrating the flow equations for a particular model is a “path” in the slow roll space parameterized by the number of e-folds N . Figures 1-3 show examples of paths plotted in the $\sigma - \epsilon$ plane for different assumptions about the central values for the parameters r , n , and $dn/d \log k$. Also plotted is the corresponding reconstructed potential for each path. Surprisingly, while quite complex behavior is possible for the slow roll parameters, this behavior is only weakly reflected in the shape of the potential itself.

IV. MONTE CARLO RECONSTRUCTION IN PRACTICE

We now describe two concrete applications of this method. First, we select central values in various regions of the observable parameter space with the error

² See Ref. [3] for a detailed discussion of the fixed-point structure of the slow roll space.

³ As usual in all analyses of inflation we ignore the back reaction of quantum fluctuations on the background evolution.

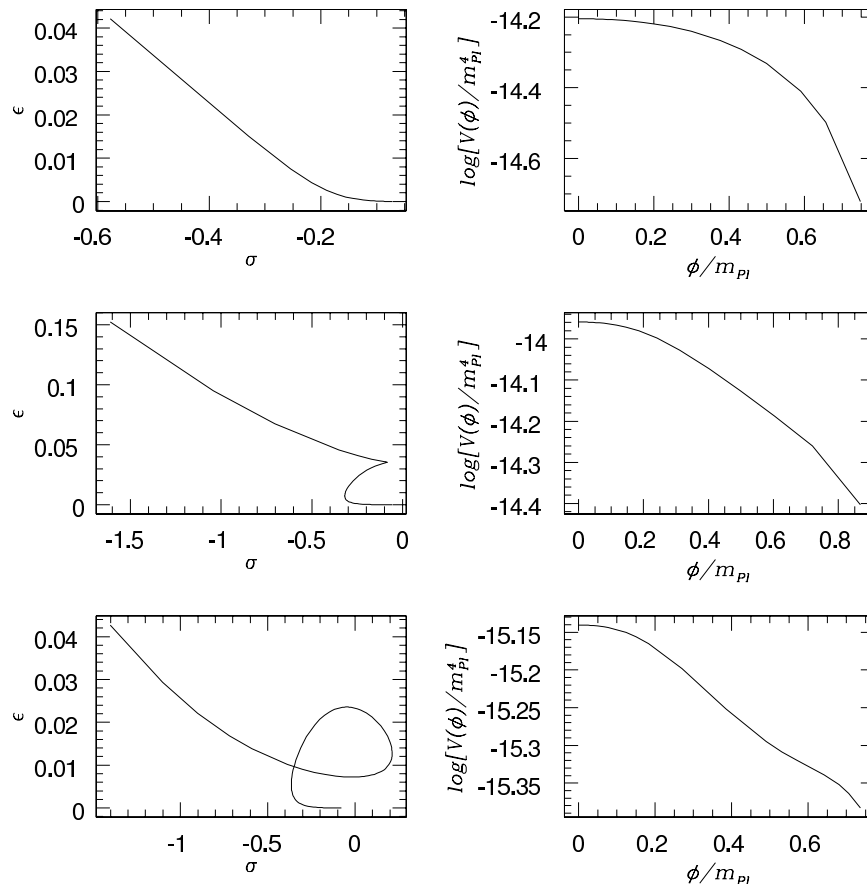


FIG. 1: Paths in the (σ, ϵ) plane (left column) and the corresponding potentials $V(\phi)$ (right column) for $r \simeq 0.0$, $n \simeq 0.93$, $dn/d\log k \simeq 0.0$.

bars expected from Planck, and reconstruct the inflationary potential based on this “synthetic” data. We find that Planck will allow us to determine the qualitative form of the potential, but is insufficiently precise for well-constrained reconstruction. This is consistent with the conclusions of other studies [1, 16]. Second, we choose a region of parameter space centered on the values for n , r and $dn/d\ln k$ for a specified potential – in this case $V(\phi) \propto \phi^4$ – and apply our reconstruction algorithm with different sized error bars, thus determining the observational precision that is needed in order to reliably reconstruct a known potential.

Figure 4 shows the results of two different “reconstructions”: for $r = 0.02$, $n = 0.95$ and $dn/d\log k = 0$, and for $r = 0$, $n = .93$ and $dn/d\log k = 0$. In both cases the errors bars are those anticipated for the Planck mission’s measurement of the spectrum [14, 22], namely $\delta r \sim 0.01$, $\delta n \sim 0.01$ and $\delta dn/d\log k \sim 0.01$. The first case has a tensor contribution that would be resolved by Planck, and the normalization of the potential is relatively tightly constrained, $V \sim 10^{-11} m_{\text{Pl}}^4$. The second reconstruction assumes that the tensor amplitude is not detectable by Planck, with a central value $r \simeq 0.0$. In this case, the normalization of the potential is very poorly constrained, although the shape of the potential is consistent with

standard “small-field” models [13]. The clear conclusion from these plots, and the other cases that we have examined, is that Planck may be able to determine the qualitative features of the potential, but it will not permit the quantitative reconstruction of the inflationary potential on its own.

It should not come as any particular surprise that Monte Carlo reconstruction does not yield a tight constraint on the possible form of the inflationary potential. However, the question this immediately raises is how much more accurately – relative to the precision expected from Planck – would we need to measure the spectrum in order to be able to make a quantitative statement about the functional form of the potential. We tackle this issue by choosing values of n , r and $dn/d\log k$ consistent with a known potential, in this case the canonical $\lambda\phi^4$ model, which is typical of “large-field” models and has a tensor fluctuation amplitude observable by Planck. With this assumption, the central values for the spectral index and tensor-to-scalar ratio are $n = 0.943$ and $r = 0.02$ (evaluated 50 e-folding before the end of inflation). For $V \propto \phi^4$, $dn/d\log k$ is close to zero, and we take the central value to be precisely zero.

Using the above choices for the central values, we have performed Monte Carlo reconstruction with Planck-

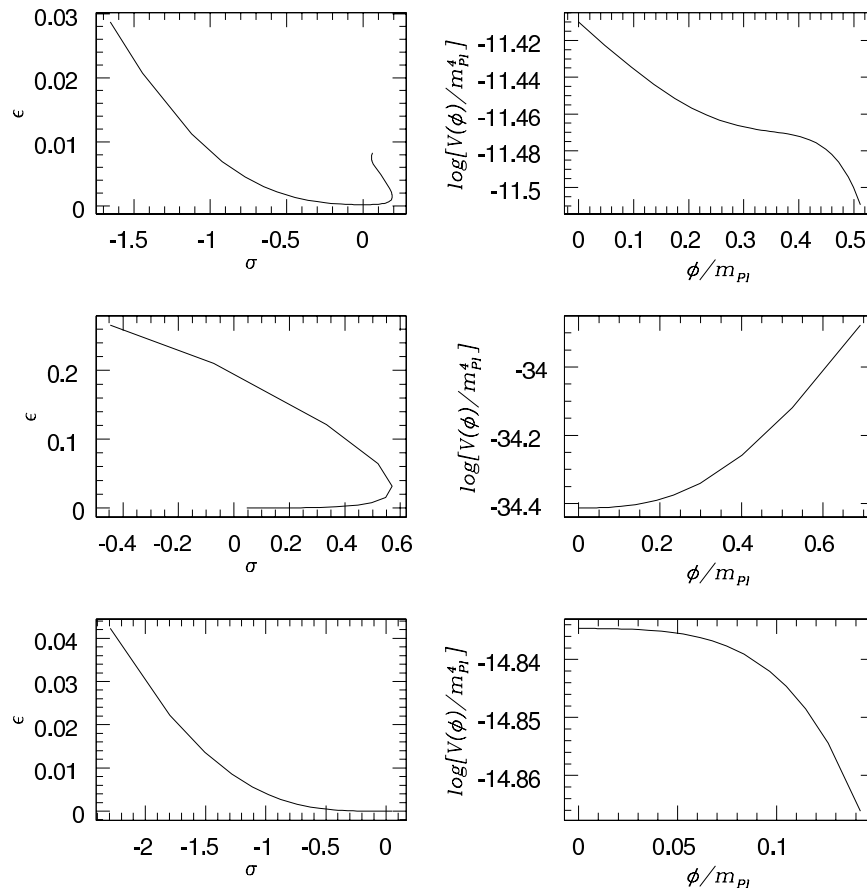


FIG. 2: Paths in the (σ, ϵ) plane (left column) and the corresponding potentials $V(\phi)$ (right column) for a blue spectrum $r \simeq 0.0$, $n \simeq 1.05$, $dn/d\log k \simeq 0.0$.

sized errors bars and with $\delta n = 0.002$, $\delta r = 0.002$ and $\delta dn/d\log k = 0.005$. The second choice leads to a box in the (n, r) plane that is 25 times smaller than the bound predicted for Planck and thus represents a substantial improvement in experimental precision. We divided the $dn/d\log k$ bound by 2 rather than 5 solely for computational convenience. The second reconstruction involved computing approximately 90 million “trial” inflationary models in order to filter out 100 solutions that passed through the specified window in parameter space. This took several days of CPU time on a fast desktop machine, and would have taken even longer if we had applied the same scaling to $\delta dn/d\log k$ as we did to δn and δr .

If we plot graphs to analogous to those in Fig. 4 for these two reconstructions we find that, unsurprisingly, the overall shape of both sets of reconstructed potentials are consistent, but that there is less spread in the set with the smaller error bars. However, to determine whether any sort of quantitative reconstruction is possible, we adopt the prior that the potentials are proportional to $(\phi - \phi_0)^m$, where ϕ_0 is an unknown offset, and then perform a least-squares fit to determine the best-fit value of m . In practice, it is sufficient to normalize the height of the reconstructed potential to precisely unity at $\phi = 0$

and then fit it to the following functional form:

$$(1 - c\phi)^m \quad (24)$$

This choice forces the fitted (and rescaled) potential to be unity when $\phi = 0$. Adding normalization as a third parameter to the fit does not have a significant impact on the computed values of m .

The results for both simulations are shown in Fig. 5. The error bars expected from the Planck mission do not allow one to conclude that $V \propto \phi^4$, but the tighter bounds on n and r do rule out values of m markedly different from 4.⁴

We thus tentatively conclude that while Planck cannot measure the perturbation spectrum accurately enough to put even mild quantitative constraints on the potential, increasing the accuracy with which both n and r can be

⁴ In reality, if the computed value of m is significantly different from 4, what we actually learn is that the potential cannot be well described by Eq. (24) – since setting m to a value significantly different from 4 produces values of n and r well outside our assumed range.

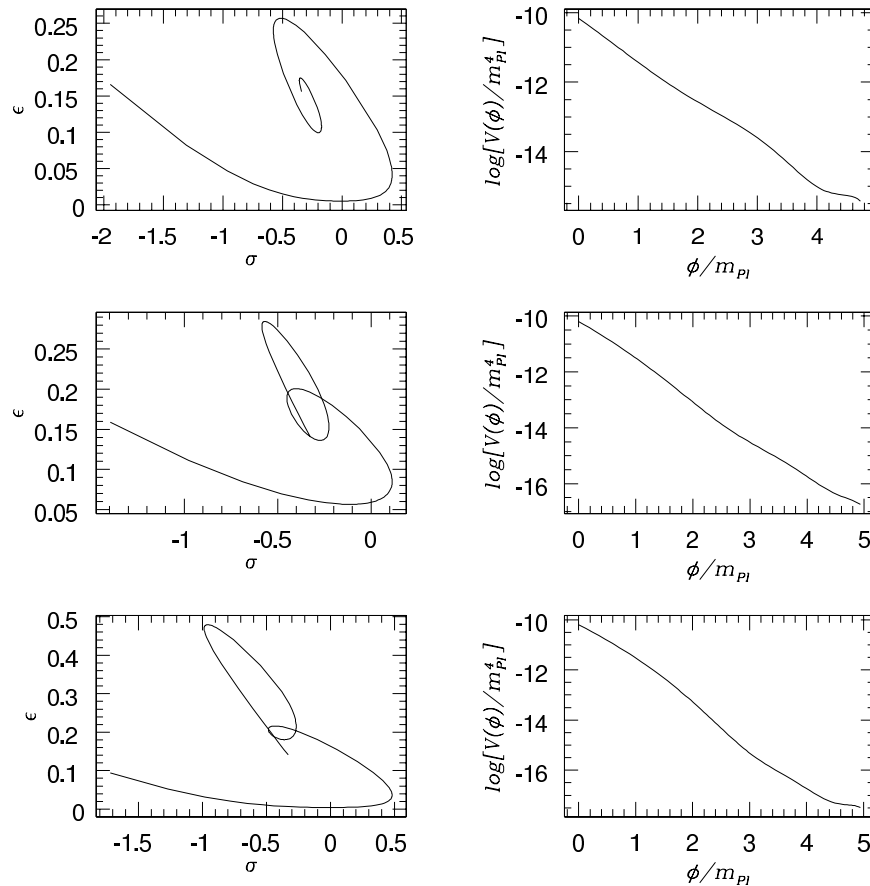


FIG. 3: Paths in the (σ, ϵ) plane (left column) and the corresponding potentials $V(\phi)$ (right column) for $r \simeq 0.18$, $n \simeq 0.6$, $dnd/\log k \simeq -0.02$. This parameter region is observationally disfavored, but shows the complicated behavior possible for solutions to the flow equations at higher order.

recovered by a factor of 5 would allow one to start making meaningful reconstructions of the potential.

V. DISCUSSION

We have presented a novel method for reconstructing the inflationary potential, based on the powerful flow equation approach to inflationary dynamics. This method, which we dub *Monte Carlo reconstruction*, differs from other prescriptions for reconstruction in that it is stochastic in nature and involves extremely weak prior assumptions about the form of the potential. A stochastic approach to reconstruction has distinct advantages compared with, for example, methods which expand the potential in a Taylor series and fit the coefficients of the Taylor expansion to observable parameters. In particular, the method can be applied equally well to both poor data sets and to high-quality data: parameters such as the tensor spectral index do not enter the reconstruction in any direct way, making the method very simple and robust. Also, Monte Carlo reconstruction naturally produces shapes for the potential outside the region directly constrained by observation. This follows from our prin-

cipal assumption, single field inflation, and the attractor behavior of the inflationary dynamics which tends to ensure that the reconstructed potentials overlap outside the region in which we have direct observational input.

We want to make clear what Monte Carlo reconstruction is *not*: it is a stochastic method, but not a statistical one. We do not have a metric on the space of initial conditions. Consequently, we cannot use the “density” of models in any particular parameter space to infer the relative likelihood of one parameter region over another. Plots of models in either the space of possible potentials or the space of exponent m (from ϕ^m , as in Fig. 5) are properly interpreted as exclusion plots, indicating which regions are either consistent or inconsistent with the data. However, we cannot determine the relative likelihood of different initial points in slow roll space without an understanding of inflationary initial conditions. Many other reconstruction attempts truncate the slow roll expansion at second or third order, but the approach here can be extended to arbitrary order in slow roll, and we have checked that our results do not depend on the specific level at which we truncate slow roll. However, any slow roll ansatz effectively rules out potentials with small features where the higher order derivatives of the potential

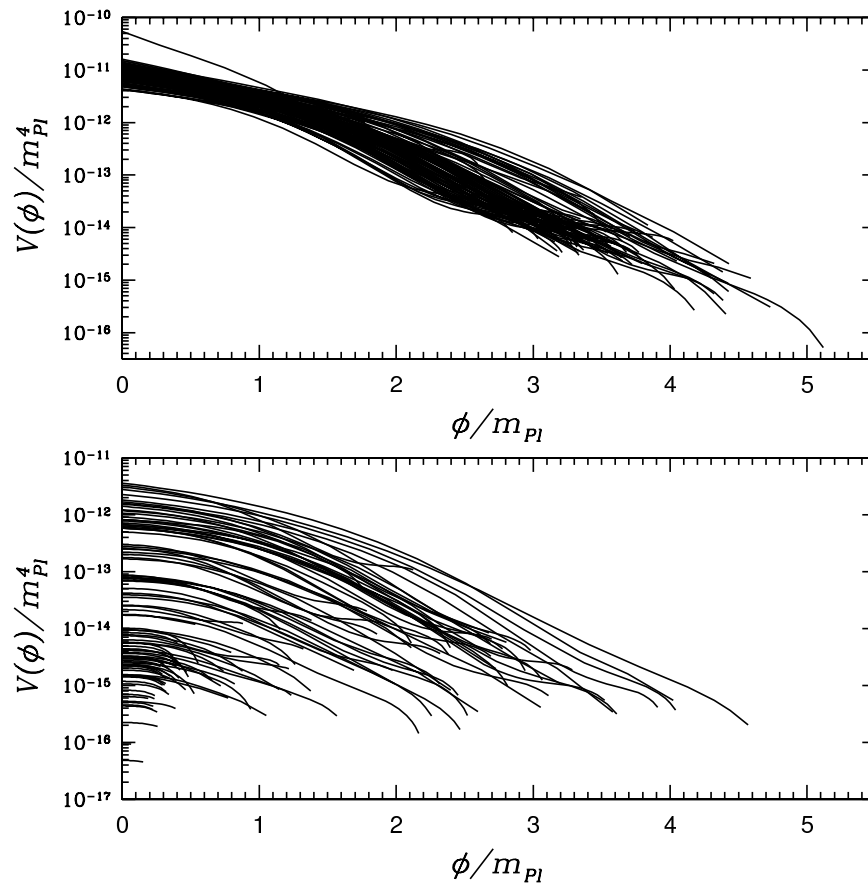


FIG. 4: The upper panel shows 100 reconstructed potentials, assuming $r = 0.02 \pm 0.01$, $n = 0.95 \pm 0.01$, $dn/d \log k = 0.0 \pm 0.01$ (the errors bars expected from the Planck mission). This choice implies that the tensor modes are unambiguously detected, and leads to a tight constraint on the normalization of the potential. The field ϕ is defined such that the observational parameters are calculated at $\phi = 0$. The lower plot shows 100 reconstructed potentials, for $r = 0.0 \pm 0.01$, $n = 0.93 \pm 0.01$, $dn/d \log k = 0.0 \pm 0.01$. In this case, tensor modes are not resolved, and the normalization of the potential is poorly constrained. The one anomalous potential in the top figure corresponds to a potential that, by chance, has comparatively large slow roll parameters, but which cancel in just the right way to produce the specified cosmological spectrum.

and $H(\phi)$ are large [23]. If the feature is located in the region of the potential that corresponds to the primordial spectrum, strict limits can be placed on the size and slope of the feature [24]. However, if the feature is outside this region then we will obviously not be able to reconstruct it.

The most straightforward application of Monte Carlo reconstruction is to simply generate an ensemble of potentials consistent with some observational constraint. This simple and robust procedure can be applied to data sets (for example the forthcoming data from the MAP satellite) for which direct functional reconstruction of the potential will likely be impossible. While this method suffers from the same fundamental limitations as any other method, it will allow us to at least answer qualitative questions about the form of the inflationary potential: for example, is the potential convex or concave? Higher quality data will allow for more quantitative constraints on the potential. Detection of a nonzero tensor component will give information about the normaliza-

tion of the potential, to within an order of magnitude or two with the accuracy projected for Planck. Even absent a detection of tensor modes, it may be possible to reach conclusions about the shape of the potential, if not its normalization. More quantitative information can be gleaned from more accurate data sets. For instance, an improvement in parameter resolution by a factor of five or so over Planck will make information about the exponent ϕ^m of the potential available in at least a rough sense. Other possible applications would be plotting the results of the Monte Carlo reconstruction in the space of derivatives of the potential, V, V', V'' , and so on, for comparison with Refs. [25, 26].

Monte Carlo reconstruction is easily generalizable. For example, one need not use the slow roll approximation to calculate the power spectrum associated with a particular choice of “slow roll” parameters generated by the flow equations. (Note that the slow roll expansion is completely distinct from the slow roll *approximation*. The solutions we generate for the background evolution are

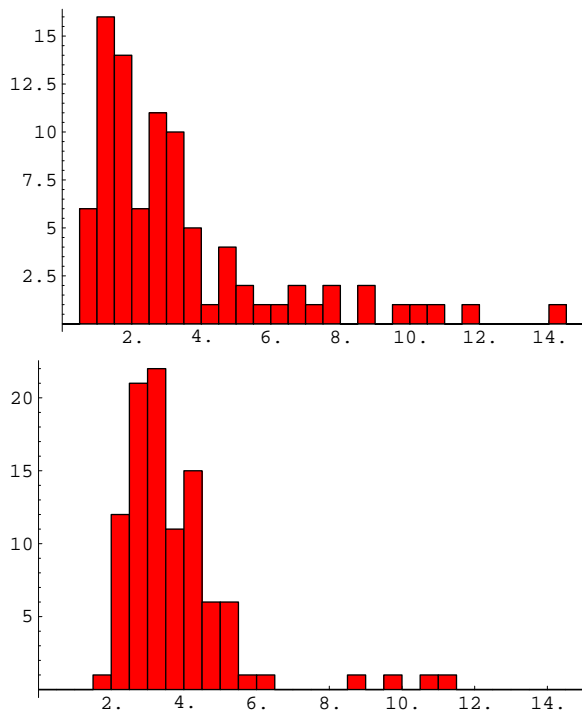


FIG. 5: These two histograms show the values of the power m (horizontal axes) obtained by fitting Eq. (24) to 100 potentials generated by the Monte Carlo reconstruction algorithm, where the measured spectra are assumed to have the central values predicted by $\lambda\phi^4$ inflation. The vertical axes indicate the number of models in a particular bin in m . In the top panel we assume that the error bars on the spectral parameters are equal to those expected from Planck, $\delta r \sim 0.01$, $\delta n \sim 0.01$ and $\delta dn/d\log k \sim 0.01$, whereas the bottom panel corresponds to $\delta r \sim 0.002$, $\delta n \sim 0.002$ and $\delta dn/d\log k \sim 0.005$. In the former case, the functional form of the potential cannot be meaningfully recovered, but in the lower case the results are consistent with $V \propto \phi^4$. In both plots we have dropped a few cases for which the least squares solver did not converge.

exact.) For calculating the fluctuation spectrum associated with a particular path in the parameter space, one could equally well apply the method of uniform approximations introduced by Habib, et al. [27]. It is also straightforward to solve for the perturbation spectrum by numerically solving the exact equation for quantum modes in the inflationary spacetime: as in the calculation of the potential itself, all the information required to do so is contained in the solution to the flow equations. Thus the method is not only exact in principle, but can be made so in practice if necessary. In addition, the same techniques could be applied to a set of flow equations based around an expansion other than the Hubble slow roll expansion of Liddle et al., such as the expansion used in Ref. [28]. Doing so would be useful to investigate the dependence of the reconstructed potentials on the details of the truncation scheme for the flow equations. We expect this dependence to be small.

Acknowledgments

RE and WHK are supported by ISCAP and the Columbia University Academic Quality Fund. ISCAP gratefully acknowledges the generous support of the Ohrstrom Foundation. We would like to thank Ed Copeland for useful discussions. RE thanks the Aspen Center for Physics, where part of this work was conducted. Some of the computational time used for these calculations were kindly provided by the High Energy Theory group at Brown University.

-
- [1] J. E. Lidsey *et al.*, Rev. Mod. Phys. **69**, 373 (1997), astro-ph/9508078.
 - [2] A. R. Liddle, P. Parsons, and J. D. Barrow, Phys. Rev. D **50**, 7222 (1994), astro-ph/9408015.
 - [3] W. H. Kinney, astro-ph/0206032.
 - [4] M. B. Hoffman and M. S. Turner, Phys. Rev. D **64**, 023506 (2001), astro-ph/0006321.
 - [5] L. P. Grishchuk and Yu. V. Sidorav, in *Fourth Seminar on Quantum Gravity*, eds M. A. Markov, V. A. Berezin and V. P. Frolov (World Scientific, Singapore, 1988).
 - [6] A. G. Muslimov, Class. Quant. Grav. **7**, 231 (1990).
 - [7] D. S. Salopek and J. R. Bond, Phys. Rev. D **42**, 3936 (1990).
 - [8] H. M. Hodges and G. R. Blumenthal, Phys. Rev. D **42**, 3329 (1990).
 - [9] E. J. Copeland et al. Phys. Rev. Lett. **71**, 219 (1993).
 - [10] E. Ayon-Beato, A. Garcia, R. Mansilla, and C. A. Terrero-Escalante, Phys. Rev. D **62**, 103513 (2000).
 - [11] E. F. Bunn, D. Scott, and M. White, Astrophys. J. Lett. **441**, L9 (1995), astro-ph/9409003.
 - [12] R. Stompor, K. M. Gorski and A. J. Banday, Mon. Not. R. Astron. Soc. **277**, 1225 (1995), astro-ph/9502035.
 - [13] S. Dodelson, W. H. Kinney, and E. W. Kolb, Phys. Rev. D **56**, 3207 (1997), astro-ph/9702166.
 - [14] W. H. Kinney, Phys. Rev. D **58**, 123506 (1998), astro-ph/9806259.
 - [15] E. D. Stewart and D. H. Lyth, Phys. Lett. **302B**, 171 (1993), gr-qc/9302019.
 - [16] I. J. Grivell and A. R. Liddle, Phys. Rev. D **61**, 081301 (2000), astro-ph/9906327.
 - [17] C. A. Terrero-Escalante, astro-ph/0209162.
 - [18] A. D. Linde, Phys. Lett. **259B**, 38 (1991).
 - [19] A. Linde, Phys. Rev. D **49** 748 (1994), astro-ph/9307002.

- [20] E. J. Copeland *et al.*, Phys. Rev. D **49**, 6410 (1994), astro-ph/9401011.
- [21] A. R. Liddle. and M. S. Turner, Phys. Rev. D **50**, 758 (1994).
- [22] E. J. Copeland, I. J. Grivell, and A. R. Liddle, Mon. Not. R. Ast. Soc. **298**, 1233 (1998), astro-ph/9702128.
- [23] L. Wang, V. F. Mukhanov, and P. J. Steinhardt, Phys. Lett. **B414**, 18 (1997).
- [24] J. Adams, B. Cresswell, and R. Easther, Phys. Rev. D **64**, 123514 (2001), astro-ph/0102236.
- [25] S. Hansen and M. Kunz, hep-ph/0109252.
- [26] C. Caprini, S. Hansen, and M. Kunz, hep-ph/0210095.
- [27] S. Habib, K. Heitmann, G. Jungmann, and C. Molina-Paris, astro-ph/0208443.
- [28] D. J. Schwarz, C. A. Terrero-Escalante, and A. A. Garcia, Phys. Lett. B **517**, 243 (2001), astro-ph/0106020.